Neuromodulator release in neurons requires two functionally redundant calcium sensors

Rhodé van Westen[a,b], Josse Poppinga[a], Rocío Díez Arazola[a], Ruud F. Toonen[a,1], and Matthijs Verhage[a,b,1]

[a]Department of Functional Genomics, Center for Neurogenomics and Cognitive Research, Neuroscience Campus Amsterdam, Vrije Universiteit Amsterdam, 1081 HV Amsterdam, The Netherlands; and [b]Department of Clinical Genetics, Amsterdam University Medical Centers, 1081 HV Amsterdam, The Netherlands

Neuropeptides and neurotrophic factors secreted from dense core vesicles (DCVs) control many brain functions, but the calcium sensors that trigger their secretion remain unknown. Here, we show that in mouse hippocampal neurons, DCV fusion is strongly and equally reduced in synaptotagmin-1 (Syt1)- or Syt7-deficient neurons, but combined Syt1/Syt7 deficiency did not reduce fusion further. Cross-rescue, expression of Syt1 in Syt7-deficient neurons, or vice versa, completely restored fusion. Hence, both sensors are rate limiting, operating in a single pathway. Overexpression of either sensor in wild-type neurons confirmed this and increased fusion. Syt1 traveled with DCVs and was present on fusing DCVs, but Syt7 supported fusion largely from other locations. Finally, the duration of single DCV fusion events was reduced in Syt1-deficient but not Syt7-deficient neurons. In conclusion, two functionally redundant calcium sensors drive neuromodulator secretion in an expression-dependent manner. In addition, Syt1 has a unique role in regulating fusion pore duration.

neuromodulators | dense core vesicles | synaptotagmin-1 | synaptotagmin-7 | hippocampal neurons

To date, over 100 genes encoding neuropeptides and neurotrophic factors, together referred to as neuromodulators, are identified, and most neurons express neuromodulators and neuromodulator receptors (1). Neuromodulators travel through neurons in dense core vesicles (DCVs) and, upon secretion, regulate neuronal excitability, synaptic plasticity, and neurite outgrowth (2–4). Dysregulation of DCV secretion is linked to many brain disorders (5–7). However, the molecular mechanisms that regulate neuromodulator secretion remain largely elusive.

Neuromodulator secretion, like neurotransmitter secretion from synaptic vesicles (SVs), is tightly controlled by Ca^{2+}. The Ca^{2+} sensors that regulate secretion have been described for other secretory pathways but not for DCV exocytosis in neurons. Synaptotagmin (Syt) and Doc2a/b are good candidate sensors due to their interaction with SNARE complexes, phospholipids, and Ca^{2+} (8–11). The Syt family consists of 17 paralogs (12, 13). Eight show Ca^{2+}-dependent lipid binding: Syt1 to 3, Syt5 to 7, and Syt9 and 10 (14, 15). Syt1 mediates synchronous SV fusion (8), consistent with its low Ca^{2+}-dependent lipid affinity (15, 16) and fast Ca^{2+}/membrane dissociation kinetics (16, 17). Syt1 is also required for the fast fusion in chromaffin cells (18) and fast striatal dopamine release (19). Synaptotagmin-7 (Syt7), in contrast, drives asynchronous SV fusion (20), in line with its a higher Ca^{2+} affinity (15) and slower dissociation kinetics (16). Syt7 is also a major calcium sensor for neuroendocrine secretion (21) and secretion in pancreatic cells (22–24). Other sensors include Syt4, which negatively regulates brain-derived neurothropic factor (25) and oxytocin release (26), in line with its Ca^{2+} independency. Syt9 regulates hormone secretion in the anterior pituitary (27) and, together with Syt1, secretion from PC12 cells (28, 29). Syt10 controls growth factor secretion (30). However, Syt9 and Syt10 expression is highly restricted in the brain (31–33). Hence, the calcium sensors for neuronal DCV fusion remain largely elusive.

Because DCVs are generally not located close to Ca^{2+} channels (34), we hypothesized that DCV fusion is triggered by high-affinity Ca^{2+} sensors. Because of their important roles in vesicle secretion, their Ca^{2+} binding ability, and their high expression levels in the brain (20, 31, 35–38), we addressed the roles of Doc2a/b, Syt1, and Syt7 in neuronal DCV fusion.

In this study, we used primary Doc2a/b-, Syt1-, and Syt7-null (knockout, KO) neurons expressing DCV fusion reporters (34, 39–41) with single-vesicle resolution. We show that both Syt1 and Syt7, but not Doc2a/b, are required for ~60 to 90% of DCV fusion events. Deficiency of both Syt1 and Syt7 did not produce an additive effect, suggesting they function in the same pathway. Syt1 overexpression (Syt1-OE) rescued DCV fusion in Syt7-null neurons, and vice versa, indicating that the two proteins compensate for each other in DCV secretion. Moreover, overexpression of Syt1 or Syt7 in wild-type (WT) neurons increased DCV fusion, suggesting they are both rate limiting for DCV secretion. We conclude that DCV fusion requires two calcium sensors, Syt1 and Syt7, that act in a single/serial pathway and that both sensors regulate fusion in a rate-limiting and dose-dependent manner.

Results

Doc2a/b Are Not Involved in DCV Fusion. To identify the calcium sensor(s) for DCV fusion in neurons, we used single hippocampal neurons cultured on glia micro islands expressing the DCV fusion reporter neuropeptide Y (NPY)-super ecliptic pHluorin (SEP) (Fig. 1 *A* and *B*) to quantify DCV fusion at single-vesicle resolution

Significance

Neuromodulators are released by most neurons and control many brain functions, but their release mechanism remains largely elusive. Calcium sensors for other secretory pathways have been characterized but not for neuromodulator release in the brain. Using release assays with single-vesicle resolution in living neurons, we identify the sensors that drive neuromodulator release from dense core vesicles. Neuromodulator release depends equally on two sensors, Syt1 and Syt7, that are both rate limiting for release and compensate for each other upon overexpression (cross-rescue), despite being in different locations in the cell. These data show that the mechanism of neuromodulator secretion is different from previously studied systems.

NEUROSCIENCE

[(34, 39, 40) see also *SI Appendix, Supplemental Methods*]. Vesicle fusion was triggered by bursts of action potentials at 50 Hz (Fig. 1*A*). The total number of DCVs per neuron was quantified upon NH_4 superfusion to dequench NPY-SEP in all DCVs (Fig. 1 *A* and *B*).

Doc2a/b are soluble high-affinity calcium sensors reported to trigger spontaneous and asynchronous SV fusion (35, 36, 38). Due to their high Ca^{2+} affinity (42), we hypothesized that Doc2a/b are suitable Ca^{2+}-sensors for DCV fusion. To test this, DCV fusion was quantified in Doc2a/b double-null (DKO) neurons and double heterozygous (DHZ) littermate controls. DCV fusion upon high frequency stimulation, visualized by rapid dequenching of NPY-SEP puncta (Fig. 1 *A* and *B*), was abundant in DHZ neurons and occurred almost exclusively during stimulation (*SI Appendix*, Fig. S1). Doc2a/b deficiency did not alter the number of DCV fusion events nor the total number of DCVs per neuron (*SI Appendix*, Fig. S1 *A* and *E*).

DCV Fusion Requires Both Syt1 and Syt7. Due to their established roles in synaptic and neuroendocrine vesicle secretion and high brain expression levels (20, 31, 33), we next tested the role of Syt1 and Syt7 using Syt1 knock-down [Syt1-KD (43)], Syt7-null mutant [Syt7-KO (44)], and Syt1-KD/Syt7-KO neurons. Immunoblotting for Syt1 confirmed Syt1-KD as shown before (*SI Appendix*, Fig. S2 *B* and *C*) (43). WT neurons showed many fusion events in response to high frequency stimulation. However, in Syt1-KD or Syt7-KO neurons, the number of fusion events was reduced by

64 and 69%, respectively (Fig. 1*C* and *SI Appendix*, Fig. S2*D*). Strikingly, loss of both Syt1 and Syt7 did not produce additive effects but a similar reduction in fusion events (76% reduction) as in single mutant neurons (Fig. 1*C* and *SI Appendix*, Fig. S2*D*). The absence of Syt1 and/or Syt7 did not significantly alter the timing of the remaining fusion events (*SI Appendix*, Fig. S2 *E* and *F*) or the total number of DCVs per neuron (Fig. 1*E*). The released fraction, defined as the number of fusing vesicles divided by the total DCV pool (Fig. 1*E*), showed a threefold reduction in Syt1-KD, Syt7-KO, and Syt1-KD/Syt7-KO neurons (Fig. 1*D*). Hence, DCV fusion in hippocampal neurons requires both Syt1 and Syt7, and loss of both sensors does not produce additive effects, suggesting that the two sensors function in a single pathway.

Syt1 and Syt7 Cross-Rescue DCV Fusion. We next asked whether the absence of one sensor can be bypassed by overexpressing the other ("cross-rescue"). To test this, Syt1 or Syt7 was overexpressed in Syt7-KO or Syt1-null mutant (Syt1-KO) (8) neurons, respectively. We first confirmed that in Syt1-KO neurons, DCV fusion was reduced to a similar extent as in Syt1-KD neurons (Fig. 2*A*). Furthermore, Syt1 re-expression in Syt1-KO neurons fully rescued DCV fusion as well as the released fraction (Fig. 2 *A* and *B*). Strikingly, overexpression of Syt7 in Syt1-KO neurons also rescued DCV fusion (Fig. 2*C*), similar to Syt1 expression. Conversely, Syt1 overexpression in Syt7-KO neurons also rescued DCV fusion to a comparable extent as Syt7 (Fig. 2 *E* and *F*). Cross-expression of either Syt1 or Syt7 did not affect the total number of DCVs
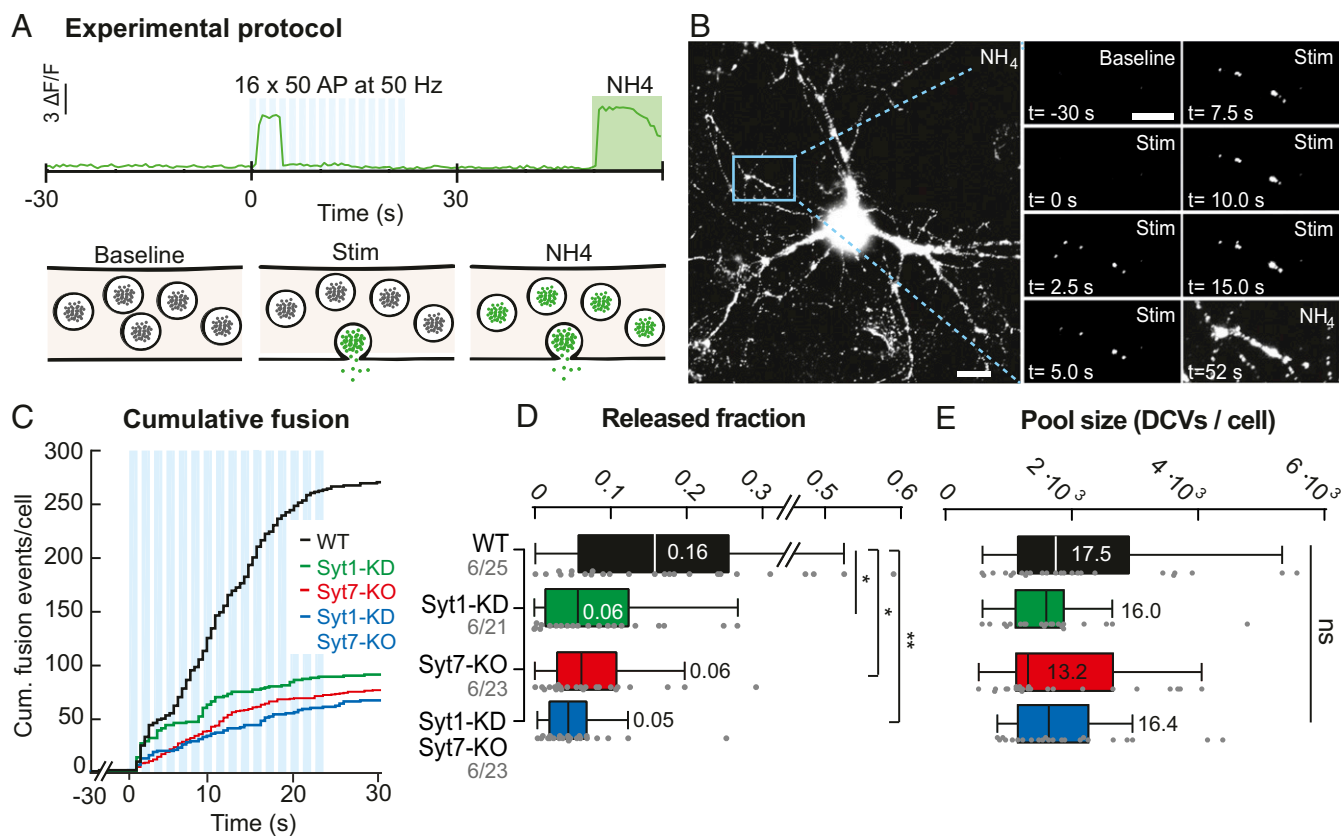
Fig. 1. Synaptotagmin-1 and synaptotagmin-7 are required for neuropeptide vesicle fusion. (*A*) Stimulation paradigm with a single vesicle fluorescence intensity trace. (*B*, *Left*) Representative image of NPY-SEP–infected neuron during Tyrode's NH_4 application. (Scale bar: 20 μm.) (*Right*) Neurite before (baseline) and during (16 × 50 AP at 50 Hz) stimulation and during NH_4 application (NH_4). (Scale bar: 10 μm.) (*C*) Median number of neuropeptide vesicle fusion events per neuron in a cumulative plot in Syt1-KD (green), Syt7-KO (red), and Syt1-KD/Syt7-KO (blue) neurons, respectively. (*D*) Fusing fraction is reduced in Syt1-KD, Syt7-KO, and Syt1-KD/Syt7-KO neurons [X^2 (4) = 14.05, P = 0.0028]. *$P < 0.05$, **$P < 0.01$, nonsignificant $P > 0.05$. (*E*) Deficiency of Syt1 or Syt7 does not affect the total number of DCVs per neuron [X^2 (4) = 1.233, P = 0.75]. The numbers before and after the dash represent the number of independent experiments/animals and the number of neurons, respectively.
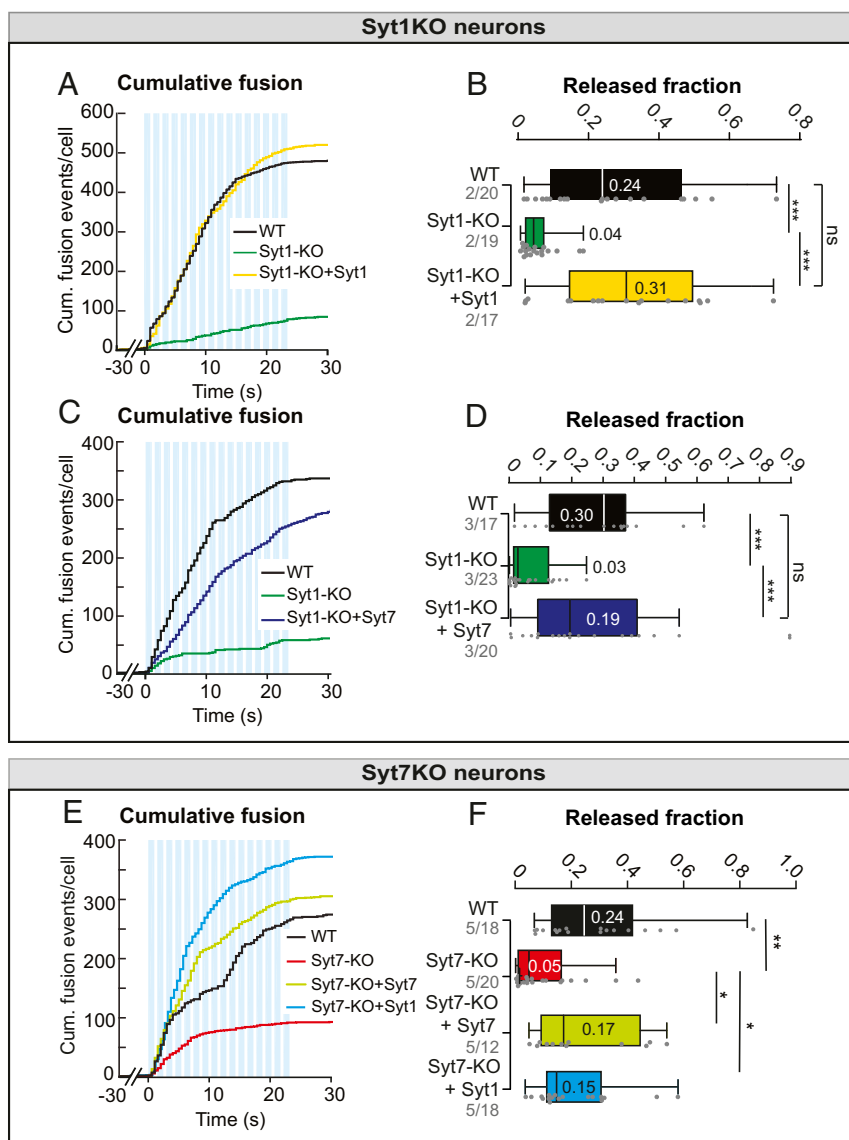
Fig. 2. Synaptotagmin-1 and synaptotagmin-7 cross-rescue neuropeptide vesicle fusion. (*A*) Median number of neuropeptide vesicle fusion events in WT, and Syt1-KO neurons with and without Syt1-OE in a cumulative plot. (*B*) Fusing fraction in Syt1-KO neurons is rescued by Syt1-OE [X^2 (3) = 19.28, $P < 0.0001$]. For lentiviral infection, 2 µL lentivirus was used. For the effects of different volumes of lentivirus, see *SI Appendix*, Fig. S4. (*C* and *D*) Same as *A* and *B* but with Syt7-OE. The fusing fraction in Syt1-KO neurons is rescued by Syt7-OE [X^2 (3) = 20.96, $P < 0.0001$]. Neurons with a fusing fraction above 0.9 were plotted at 0.9 for visualization purposes. (*E* and *F*) Same as *A* and *B* but with Syt7-KO neurons with Syt7-OE and Syt1-OE. The fusing fraction in Syt7-KO neurons is rescued by Syt7-OE and Syt1-OE [X^2 (4) = 15.96, $P = 0.0012$]. *$P < 0.05$, **$P < 0.01$, ***$P < 0.001$, nonsignificant $P > 0.05$. The numbers before and after the dash represent the number of independent experiments/animals and the number of neurons, respectively.
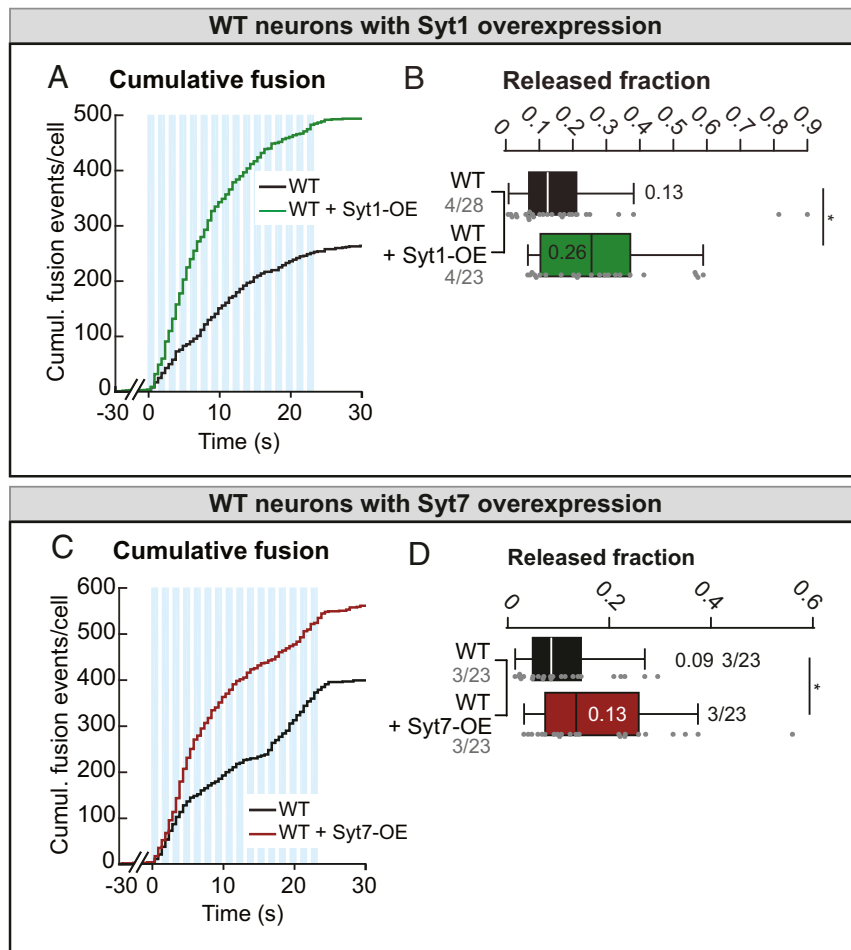
(*SI Appendix*, Fig. S3 *A–C*). Hence, Syt1 and Syt7 are functionally redundant in supporting DCV fusion upon overexpression.

Overexpression of Syt1 and Syt7 in WT Neurons Increases DCV Fusion. The cross-rescue data suggest that endogenous Syt1/7 levels are rate limiting for DCV fusion. To confirm this, Syt1 and Syt7 were overexpressed in WT neurons. Overexpression resulted in a 50 and 100% increase in Syt1 and Syt7 immunostaining intensity, respectively, without affecting the expression of the other sensor (*SI Appendix*, Fig. S5 *C* and *D*). Total DCV pool sizes were unaffected (*SI Appendix*, Fig. S5 *A* and *B*). Overexpressing Syt1 (Fig. 3*A*) or Syt7 (Fig. 3*C*) in WT neurons increased DCV fusion and the released fraction twofold and 1.5-fold, respectively (Fig. 3 *B* and *D*). These data suggest that endogenous levels of Syt1 and Syt7 are indeed both rate limiting for DCV fusion in neurons.

Syt1, and to a Lesser Extent Syt7, Are Present on Traveling and Fusing DCVs. The lack of additive effect in Syt1-KD/Syt7-KO neurons (Fig. 1) suggests that Syt1 and Syt7 operate in a single pathway. Therefore, we tested where in the neuron Syt1 and Syt7 are located and specifically whether both are present on DCVs. First, we tested colocalization of endogenous Syt1/7 with NPY-SEP in neurites. Colocalization is expressed by the Manders M1/M2 coefficient, which reports the co-occurring fraction of color 1 with color 2 and ranges from 0 (no overlap) to 1 (complete overlap). Syt1 and VGluT1 largely colocalized (VGlut1:Syt1 = 0.83 and Syt1:VGluT1 = 0.70, *SI Appendix*, Fig. S6 *A* and *B*), in line with Syt1's presence on SVs (45–47). However, Syt1 puncta were also observed extrasynaptically (Fig. 4*A* and *SI Appendix*, Fig. S6*A*) and highly colocalized with NPY-SEP (Manders NPY:Syt1 = 0.72, Syt1:NPY = 0.62; Fig. 4 *A* and *B*). NPY:Syt1 colocalization was significantly higher than NPY:VGluT1 (Fig. 4*B*, Manders

van Westen et al.
Neuromodulator release in neurons requires two functionally redundant calcium sensors

PNAS | 3 of 12
https://doi.org/10.1073/pnas.2012137118

Fig. 3. Overexpression of Syt1-OE and Syt7-OE in WT neurons increases neuropeptide vesicle fusion. (*A*) Median number of neuropeptide vesicle fusion events in WT neurons with and without Syt1-OE in a cumulative plot. (*B*) Fusing fraction is increased in WT neurons with Syt1-OE (Mann–Whitney $U = 193$, $P < 0.05$). Neurons with a fusing fraction above 0.9 were plotted at 0.9 for visualization purposes. (*C* and *D*) Same as *A* and *B* but with Syt7-OE (Mann–Whitney $U = 174$, $P < 0.05$). *$P < 0.05$, nonsignificant $P > 0.05$. The numbers before and after the dash represent the number of independent experiments/animals and the number of neurons, respectively.

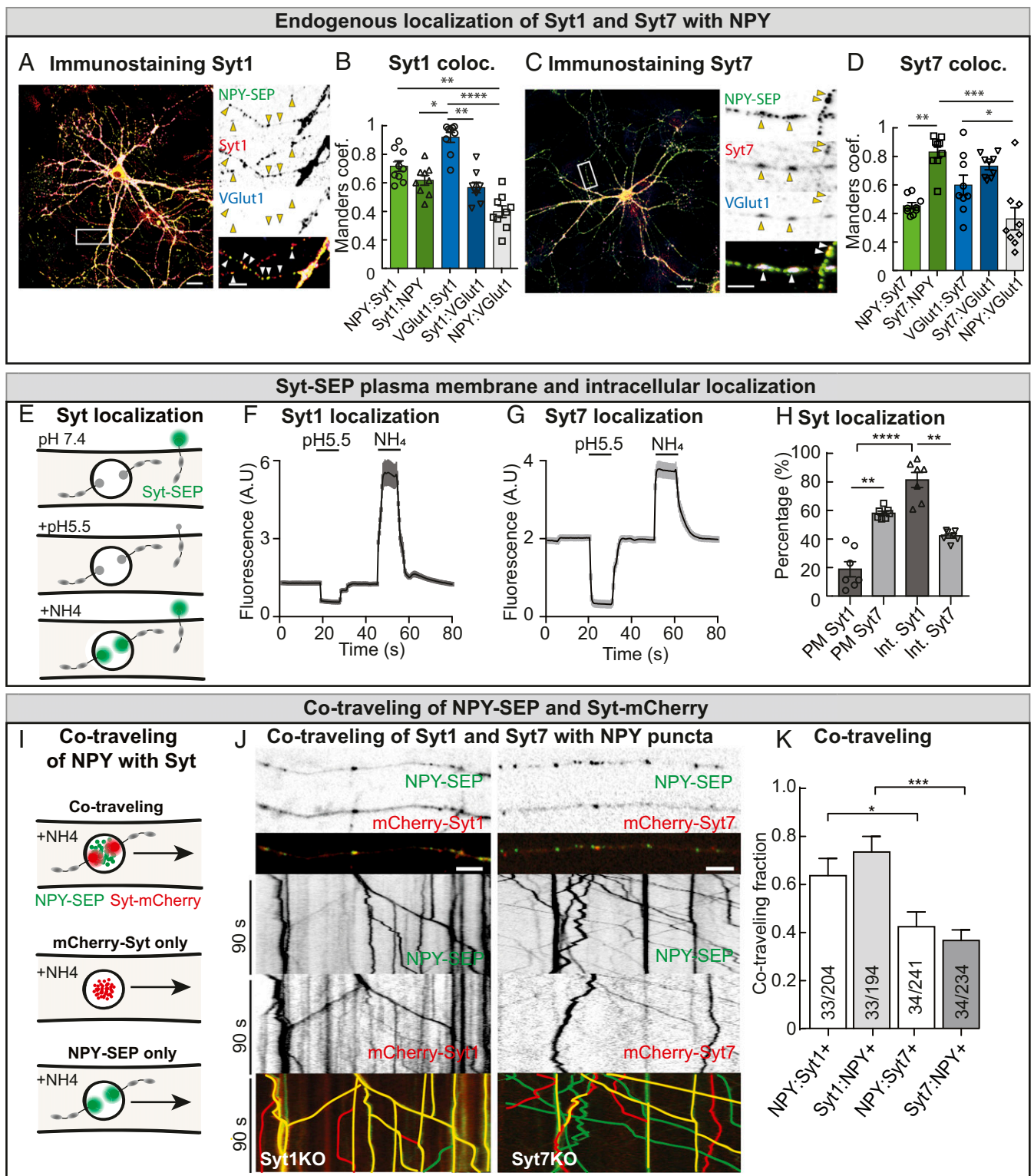NPY:VGlut1 = 0.40 and 0.36 in Syt1KO and Syt7KO neurons, respectively).

NPY-SEP colocalized only partially with Syt7 (Manders coefficient = 0.45, Fig. 4 *C* and *D*), but Syt7 showed large overlap with both NPY-SEP and the synaptic vesicle marker VGluT1 (Manders coefficient = 0.83 and 0.73, respectively). Hence, Syt7 localizes to presynaptic terminals and colocalizes with some extrasynaptic DCVs. Together, this suggests that DCVs colocalize with Syt1 and to a lesser extent with Syt7.

Next, we expressed Syt1 or Syt7 fused to SEP, expected to be at the luminal side of DCVs as described for SVs (10). In this way, plasma membrane–targeted Syt1/7-SEP is quenched by application of acidic solution, and DCV-targeted Syt1/7-SEP is dequenched by NH$_4$. Hence, acid and NH$_4$ washes probe the plasma membrane and vesicular fraction of Syt1/7-SEPs, respectively (Fig. 4*E*). Syt1-SEP was primarily on acidic intracellular locations, with only ±20% on the plasma membrane (Fig. 4 *F* and *H*), in line with previous reports (48–50). Syt7-SEP localized predominantly to the plasma membrane, and ±40% was localized to acidic intracellular compartments (Fig. 4 *G* and *H*), also in line with previous reports (48, 49, 51). These results suggest that Syt1 is primarily targeted to secretory vesicles, while Syt7 is largely targeted to the plasma membrane.

To confirm if Syt1 (and Syt7 to some extent) is indeed targeted to DCVs, we tested co-traveling of Syt1/7-mCherry fusion constructs with NPY-SEP, visualized by NH4 superfusion (Fig. 4*I*). In contrast
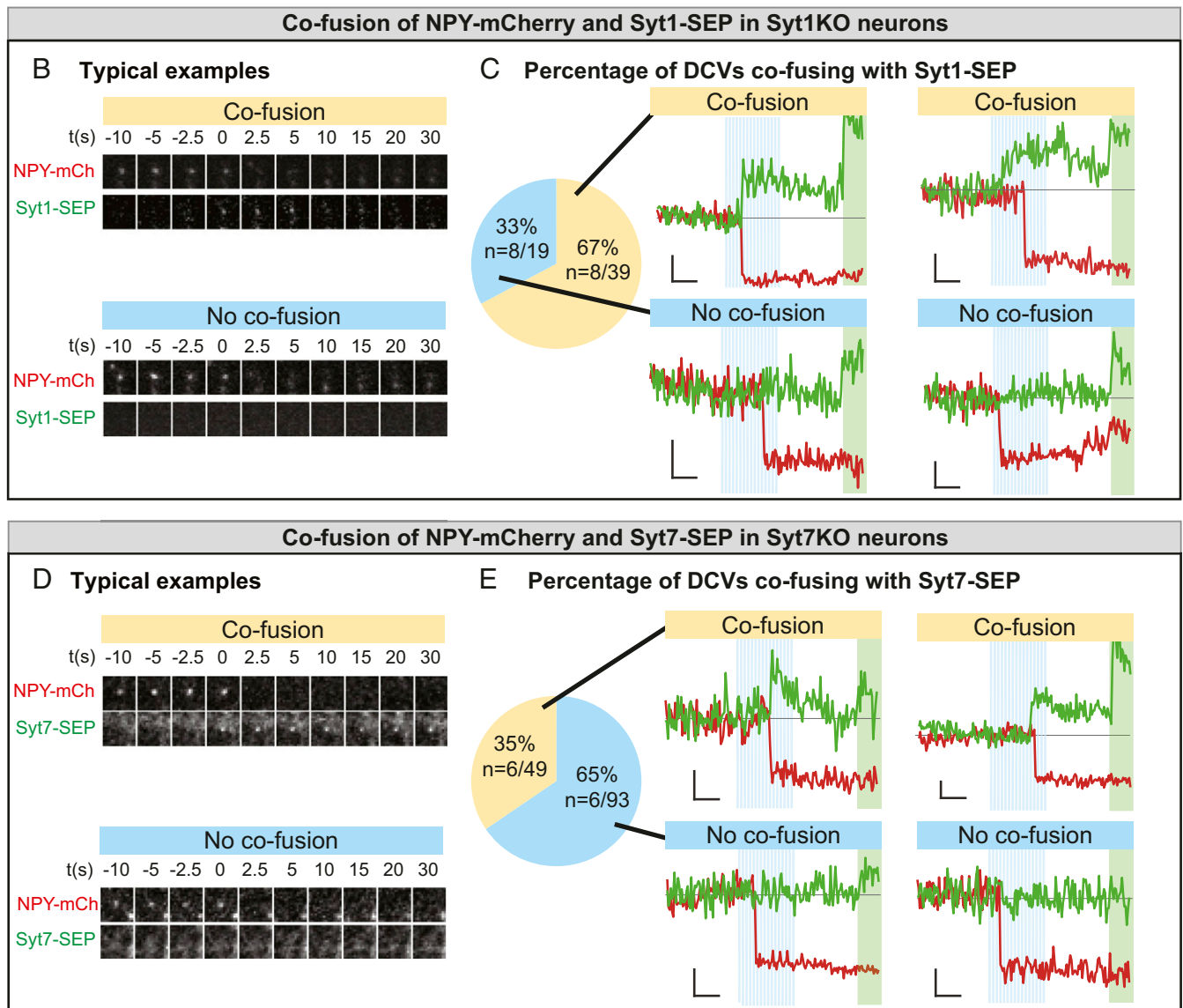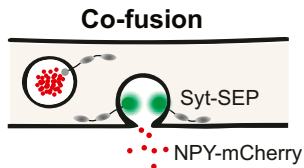
to colocalization analysis (Fig. 4 *A–D*), co-traveling analysis only includes moving puncta/vesicles. We first confirmed that the Syt-mCherry constructs fully rescued DCV fusion in Syt1-KO and Syt7-KO neurons, respectively (*SI Appendix*, Fig. S7 *A–F*). Next, we tested their co-traveling with NPY-SEP (Fig. 4 *J* and *K*). The DCV marker traveled together with Syt1-mCherry in $64 \pm 3\%$ of cases and to a lesser extent with Syt7 ($42 \pm 4\%$, Fig. 4 *J* and *K*). These data suggest that Syt1 localizes to DCVs, and Syt7 also, but to a lesser extent.

To test whether Syt1 and Syt7 are present on fusing DCVs, Syt1-SEP or Syt7-SEP were co-expressed with NPY-mCherry in Syt1-KO or Syt7-KO neurons, respectively (Fig. 5*A*), together with Synapsin-enhanced cyan fluorescent protein (ECFP) as a synapse marker. NPY-mCherry is a red DCV fusion reporter that detects DCV cargo release (52) (in contrast to NPY-SEP, which detects fusion pore opening, see *SI Appendix, Supplemental Methods*). DCV fusion events are defined as the (sudden) disappearance of NPY-mCherry puncta, and corresponding Syt1/7-SEP dequenching in the same location was quantified. Syt1-SEP fluorescence increased upon stimulation at Synapsin-ECFP–labeled synapses, most likely because of Syt1-SEP expression on SVs (*SI Appendix*, Fig. S8*E*). Therefore, only extrasynaptic NPY-mCherry fusion events were analyzed for Syt1-SEP dequenching. Syt1-SEP dequenching directly preceded NPY-mCherry loss in 67% of the events (Fig. 5 *B* and *C* and *SI Appendix*, Fig. S8*C*), suggesting that the majority of fusing DCVs express Syt1-SEP.

4 of 12 | PNAS
https://doi.org/10.1073/pnas.2012137118

van Westen et al.
Neuromodulator release in neurons requires two functionally redundant calcium sensors

Fig. 4. Syt1, and to lesser extent Syt7, colocalizes and co-travels with NPY-mCherry. (*A*) Representative image of neuron immunostained for Syt1, NPY-SEP, and VGluT1. (Scale bars: large image: 20 µm; zoomed image: 5 µm.) To detect extrasynaptic Syt1, higher laser powers were required than for synaptic Syt1 detection (*SI Appendix*, Fig. S6 *A* and *B*). (*B*) Quantification of colocalization between Syt1, NPY-SEP, and VGluT1 [X^2 (5) = 31.74, $P < 0.0001$]. (*C*) Representative image of neuron immunostained for Syt7, NPY-SEP, and VGluT1. (Scale bars: large image: 20 µm; zoomed image: 5 µm.) (*D*) Quantification of colocalization between Syt7, NPY-SEP, and VGluT1 [X^2 (5) = 25.25, $P < 0.0001$]. (*E*) Cartoon of Syt-SEP, localized at the plasma membrane or at acidic intracellular compartments, at a neutral pH (7.4) and during bath application of acidic pH (pH 5.5) or NH$_4$-contaning imaging solution. (*F* and *G*) Average Syt1-SEP (*n* = 7 cells) (*F*) and Syt7-SEP (*n* = 7 cells) (*G*) fluorescence response during bath application of pH 5.5 or 50 mM NH$_4$ Tyrode's solution. (*H*) Quantification of plasma membrane/intracellular fraction of Syt1-SEP and Syt7-SEP [X^2 (4) = 24.56, $P < 0.0001$]. (*I*) Cartoon of co-traveling of NPY-mCherry and Syt-SEP vesicles. (*J*) mCherry-Syt1 and mCherry-Syt7 partially co-travel with NPY-SEP vesicles. (Scale bars: 5 µm.) (*K*) Quantification of co-traveling of NPY with Syt1-SEP or Syt7-SEP and vice versa [X^2 (4) = 19.47, $P < 0.0002$]. The numbers before and after the dash represent the number of neurites and the number of trafficking vesicles, respectively. *$P < 0.05$, **$P < 0.01$, ***$P < 0.001$, ****$P < 0.0001$, nonsignificant $P > 0.05$.

van Westen et al.
Neuromodulator release in neurons requires two functionally redundant calcium sensors

PNAS | 5 of 12
https://doi.org/10.1073/pnas.2012137118

A Cofusion with NPY-mCherry and Syt-SEP

Co-fusion

Co-fusion of NPY-mCherry and Syt1-SEP in Syt1KO neurons

B Typical examples

C Percentage of DCVs co-fusing with Syt1-SEP

Co-fusion of NPY-mCherry and Syt7-SEP in Syt7KO neurons

D Typical examples

E Percentage of DCVs co-fusing with Syt7-SEP

Fig. 5. Fusing NPY-mCherry vesicles colocalize with Syt1-SEP and to lesser extent with Syt7-SEP events. (*A*) Schematic representation of NPY-mCherry events co-fusing with Syt-SEP. (*B*) Representative images of fusing NPY-mCherry with and without increase of Syt1-SEP. (*C*) Percentage of colocalization of fusing NPY-mCherry events (red lines of typical example traces) with sudden appearance of Syt1-SEP (green lines of typical example traces). *n* represents the number of cells and the number of extrasynaptic NPY fusion events. Synapses were defined by an accumulation of VGluT1 vesicles/above threshold VGluT1 fluorescence. Fusion events that do not overlap with these VGluT1 accumulations were considered extrasynaptic. (*D*) Representative images of fusing NPY-mCherry with and without increase of Syt7-SEP. (*E*) Same as *C* but with Syt7-SEP. *n* represents the number of cells and the number of NPY fusion events. The numbers before and after the dash represent the number of neurons and the number of DCVs, respectively. Scale bars represent 10 s (*x*-axis) and 0.2 ΔF/F (*y*-axis).

We next tested whether Syt7-SEP localizes to fusing DCVs. In $35 \pm 0.05\%$ of the fusion events, Syt7-SEP dequenching (Fig. 5 *D* and *E*) preceded NPY-mCherry loss (Fig. 5 *D* and *E* and *SI Appendix,* Fig. S8*D*). These events occurred at Synapsin-ECFP–labeled synapses and outside synapses (*SI Appendix,* Fig. S8*A*). Hence, the majority of fusion events (with cargo release) do not express Syt7-SEP. Together, these data suggest that Syt1 is present on traveling and fusing DCVs, while Syt7 regulates DCV fusion primarily from another location, probably the plasma membrane.

Syt1, but Not Syt7, Drives Fusion Pore Duration. Syt1 and Syt7 regulate fusion pore dilation and stability in PC12 and chromaffin cells (53–57). To test this in neurons, the duration of single fusion events was assessed in all genotypes. The duration was defined as

6 of 12 | PNAS
https://doi.org/10.1073/pnas.2012137118

van Westen et al.
Neuromodulator release in neurons requires two functionally redundant calcium sensors

the time between the onset of NPY-SEP dequenching, indicating fusion pore opening, and return to baseline levels, indicating either a) fusion pore closure followed by vesicle reacidification ("kiss-and-run") or b) complete DCV cargo release ("full fusion") followed by cargo diffusion in extracellular space (41) (Fig. 6 *A* and *B*). Fusion event duration varies over a wide range (*SI Appendix*, Fig. S2*A*) (58), probably because of a1) variable fission efficiency for kiss-and-run events, a2) variable expression of proton pumps per DCV, b1) variable cargo condensation limiting diffusion out of DCVs, and b2) cargo binding to the extracellular matrix limiting diffusion after full vesicle collapse (41). These factors were considered a constant among genotypes.

In WT neurons, fusion events lasted for 12.0 ± 1.3 s (Fig. 6 *D*, *F*, and *H*). In Syt1-KO, the median duration was significantly shorter, 5.5 s (Fig. 6 *C–F*), and rescued by Syt1 overexpression (16.5 s, Fig. 6 *C* and *D*). In contrast, Syt7-OE did not rescue the shorter event duration in Syt1-KO neurons (5.4 s, Fig. 6 *E* and *F*). In Syt7-KO, Syt7-KO + Syt7-OE, and Syt7-KO + Syt1-OE neurons, fusion event duration was normal (Fig. 6 *G* and *H*). Together, these data suggest that Syt1, but not Syt7, regulates fusion event duration.

Fusion timing, defined as the latency to fusion onset relative to the onset of stimulation, was not significantly different between all groups tested (*SI Appendix*, Fig. S3 *D–F*). Given existing evidence for specific roles of Syt1/7 during initial phases of release (8, 18, 20, 21), we compared the percentage of vesicles that fused during the first 50 action potentials (AP), or during the first 150 AP, and found no differences (*SI Appendix*, Fig. S9 *A–D* and *F*, respectively). Finally, the relative number of delayed fusion events, after the end of the stimulation, was also not significantly different (*SI Appendix*, Fig. S10 *B, D, F, and H*). Hence, Syt1 and Syt7 do not affect the timing of DCV fusion events.

Syt1 Is Rate Limiting for Fusion Pore Regulation. To test whether Syt1 is also rate limiting for fusion pore duration (as for fusion triggering), we assessed if Syt1 overexpression in WT neurons increases fusion event duration. Indeed, Syt1 overexpression prolonged event duration (Fig. 7 *A* and *B*), whereas Syt7 overexpression did not (Fig. 7 *C* and *D*). This suggests that endogenous levels of Syt1, but not Syt7, are rate limiting for the regulation of fusion pore duration. Finally, we tested whether the transmembrane (TM) domain of Syt1 is required for fusion event duration by expressing GAP43-Syt1/7, Syt1/7 mutants lacking their TM domains and instead containing a palmitoylation site that localizes these constructs to the plasma membrane (59, 60) (*SI Appendix*, Fig. S11 *A*, *B*, *G*, and *H*). GAP43-Syt1 expression rescued DCV fusion in Syt1-KO neurons (*SI Appendix*, Fig. S11 *C* and *D*) but failed to prolong event duration (*SI Appendix*, Fig. S11 *E* and *F*). In contrast, GAP43-Syt7 did not rescue DCV fusion in Syt7-KO neurons and did not alter event duration (*SI Appendix*, Fig. S11 *I–L*). These data indicate that Syt7, unlike Syt1, requires its TM domain to support DCV fusion and that Syt1 requires its TM domain to regulate fusion pore duration (either for functional protein formation and/or correct targeting).

DCV Fusion Requires the Ca^{2+}-Binding Capacity of Syt1 and Syt7. To confirm whether Syt1 and Syt7 are indeed Ca^{2+} sensors for DCV fusion, we expressed Syt1 and Syt7 variants that cannot bind Ca^{2+} [Syt1-DA and Syt7-DA (20)] in Syt1KO or Syt7KO neurons. Overexpression of Syt1-DA and Syt7-DA did not restore DCV fusion (*SI Appendix*, Fig. S12 *A, B, E, and F*) in Syt1KO or Syt7KO neurons, respectively. Similarly, the shortened event duration observed in Syt1-KO neurons was not rescued by overexpression of Syt1-DA (*SI Appendix*, Fig. S12 *C* and *D*). These data suggest that Ca^{2+} binding is indeed required for Syt1/7-dependent DCV fusion, and both Syt1 and Syt7 are main Ca^{2+} sensors for DCV fusion.
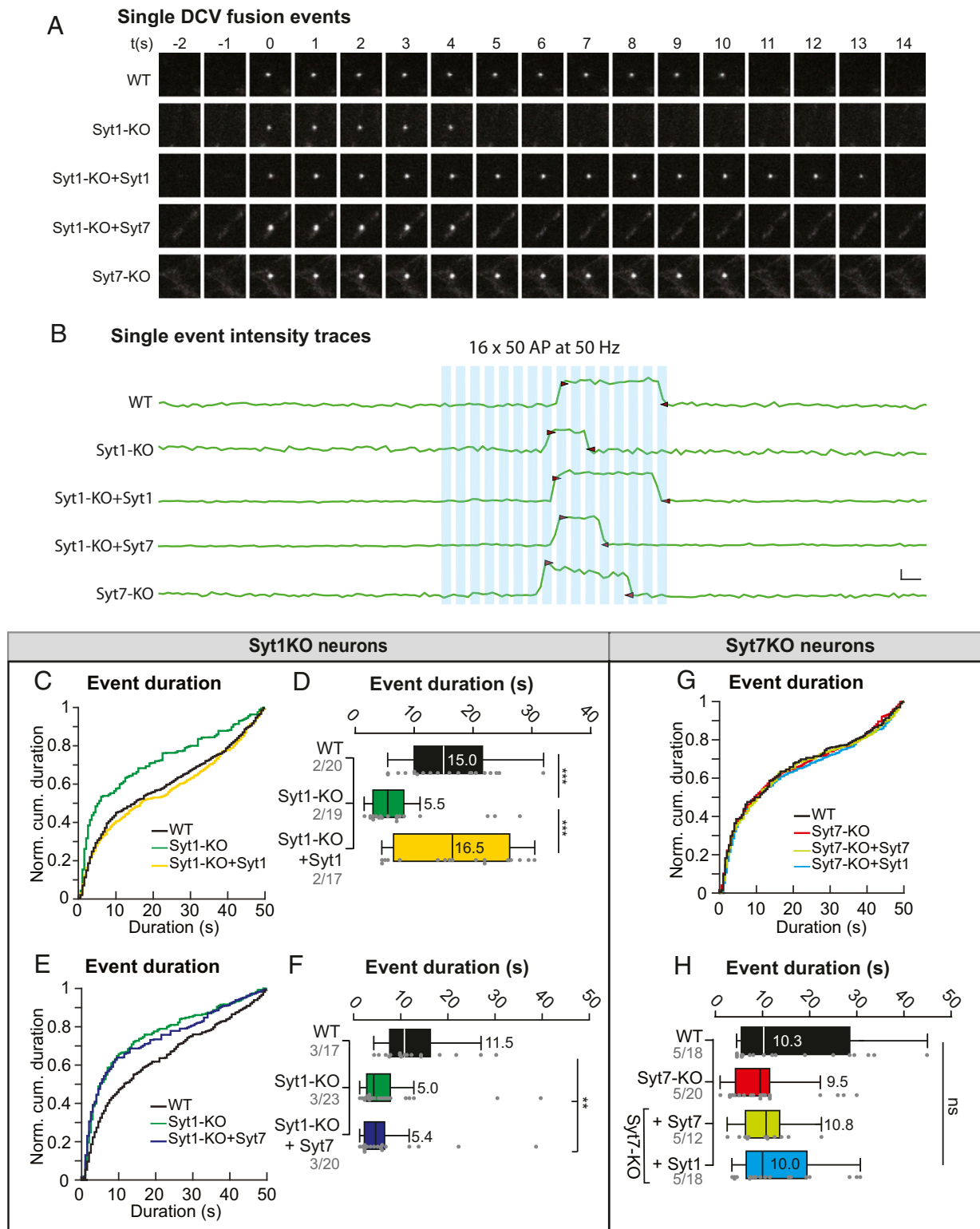
Discussion

Calcium sensors have been identified for fusion of SVs (8, 20), lysosomes (61), secretory granules in pancreatic α- and β-cells (22, 23, 62, 63), and in neuroendocrine cells (18, 21). However, the calcium sensors responsible for neuromodulator release in most neurons remained largely unknown. In this study, we show that in hippocampal neurons, Syt1 or Syt7 deficiency, but not DOC2A/B deficiency, each reduced DCV fusion by 60 to 90% (Figs. 1 *C* and *D* and 2 *A–F* and *SI Appendix*, Figs. S1 *A* and *E*, S4 *D–I*, S7 *A–F*, S11 *A –I*, and S12 *A–H*). Syt1 or Syt7 deficiency did not selectively affect specific components of DCV fusion (*SI Appendix*, Figs. S2*F*, S3 *D–F*, and S9) but affected fusion equally (Fig. 1 *C* and *D*), and the deficiency of both did not produce additive effects (Fig. 1 *C* and *D* and *SI Appendix*, Fig. S2*D*). This indicates that, in hippocampal neurons, Syt1 and Syt7 together drive fusion of the same vesicle pool with the same kinetics in a single secretory pathway. This situation is different from the best studied systems so far, where sensors have specialized functions and drive fusion of distinct release phases: Syt1 drives synchronous SV fusion in neurons and fast secretory granule fusion in chromaffin cells, while Syt7 primarily drives asynchronous and slow fusion in these two systems (8, 18, 20, 21) and may be involved in vesicle priming (20, 21) and activity-dependent pool replenishment (49). Syt7 overexpression does not restore (Syt1-driven) synchronous SV release in Syt1-KO neurons (20), and the combined deficiency of Syt1 and Syt7 reduces both phases, producing clear additive effects (20, 21). Hence, while Syt1 and Syt7 have clearly specialized functions in SV and chromaffin granule exocytosis, they do not for DCVs. This difference may be explained by evolutionary adaptations, optimizing chromaffin granule and SV exocytosis for fast/ultrafast kinetics, while there may not be an evolutionary advantage for optimizing neuromodulator signaling further. Syt1 and Syt7 most likely emerged by gene duplication of an ancestral Syt. Our data suggest that this duplication happened first, making secretory pathways more efficient and stimulus dependent, and that Syt1 and Syt7 subsequently became more specialized to drive different phases of fast or ultrafast vesicle fusion in highly specialized secretory pathways but not in the DCV pathway. Although our data indicate that Syt1 and Syt7 do not have specialized functions in DCV exocytosis, their contributions are not equal, for example, Syt1 overexpression rescues fusion better than Syt7, and Syt1 supports DCV fusion when anchored in DCVs or the plasma membrane, but this is unclear for Syt7.

DCV fusion is not completely abolished in Syt1- and Syt7-deficient neurons (Fig. 1 *C* and *D*), suggesting other calcium sensors regulate DCV fusion. Syt3 and Syt5 are the best candidates to support these remaining events as they mediate Ca^{2+}-dependent liposome fusion (14), bind SNARE proteins (64), and are expressed in the hippocampus (31, 33).

Although Syt1 and Syt7 have specialized functions in synaptic transmission, but not in the DCV secretory pathway, the two sensors appear to act on a single pool of vesicles in both situations. Functional redundancy among Syts has been shown for the maintenance of the readily releasable vesicle pool (65), and Syt7 overexpression inhibits the increase of spontaneous SV fusion in Syt1-deficient neurons (20). Hence, with or without specialized functions, the two sensors do not act in parallel pathways but drive fusion of a single pool of vesicles in a single pathway for SVs and DCVs alike.

Neuromodulator signaling is a slow process relative to synaptic transmission, and DCV fusion requires prolonged stimulation with very few DCVs fusing upon single AP stimulation (34) and during the onset of high frequency stimulation (*SI Appendix*, Fig. S9 *A–C*). The key determinants of these slow kinetics remain incompletely understood, but one relevant observation is that DCVs, unlike SVs, do not typically cluster at the active zone (39, 66), where

van Westen et al.
Neuromodulator release in neurons requires two functionally redundant calcium sensors

PNAS | 7 of 12
https://doi.org/10.1073/pnas.2012137118

Fig. 6. Synaptotagmin-1, but not Syt7, is required for event duration. (*A*) Representative images of NPY-SEP events. (*B*) Representative fluorescence traces of NPY-SEP event ROIs. The duration was defined as the time between the onset of NPY-SEP (baseline fluorescence + 2 SD) and return to baseline levels. Scale bar represents 2 s (*x*-axis) and 1 ΔF/F (*y*-axis). (*C*) Normalized cumulative median event duration per neuron in WT, Syt1-KO, and Syt1-KO neurons with Syt1-OE. For lentiviral infection, 2 μL lentivirus was used. For the effects of different volumes of lentivirus, see *SI Appendix*, Fig. S4. (*D*) Event duration in Syt1-KO neurons is rescued by Syt1-OE [X^2 (3) = 13.27, *P* = 0.0013]. (*E*) Normalized cumulative median event duration per neuron in WT, Syt1-KO, and Syt1-KO neurons with Syt7-OE. (*F*) Event duration in Syt1-KO neurons is not rescued by Syt7-OE [X^2 (3) = 13.28, *P* = 0.0013]. (*G*) Normalized cumulative median event duration per neuron in WT neurons, Syt7-KO, and Syt7-KO neurons with Syt7-OE. (*H*) Event duration is unaltered in Syt7-KO neurons with Syt1-OE and Syt7-OE [X^2 (4) = 1.475, *P* = 0.67]. All data presented in this figure corresponds to data presented in Fig. 2. The numbers before and after the dash represent the number of independent experiments/animals and the number of neurons, respectively. **$P < 0.01$, ***$P < 0.001$, nonsignificant $P > 0.05$. The text refers to a WT event duration of 12.0 ± 1.3 s, computed over all three experiments, for representative purposes.
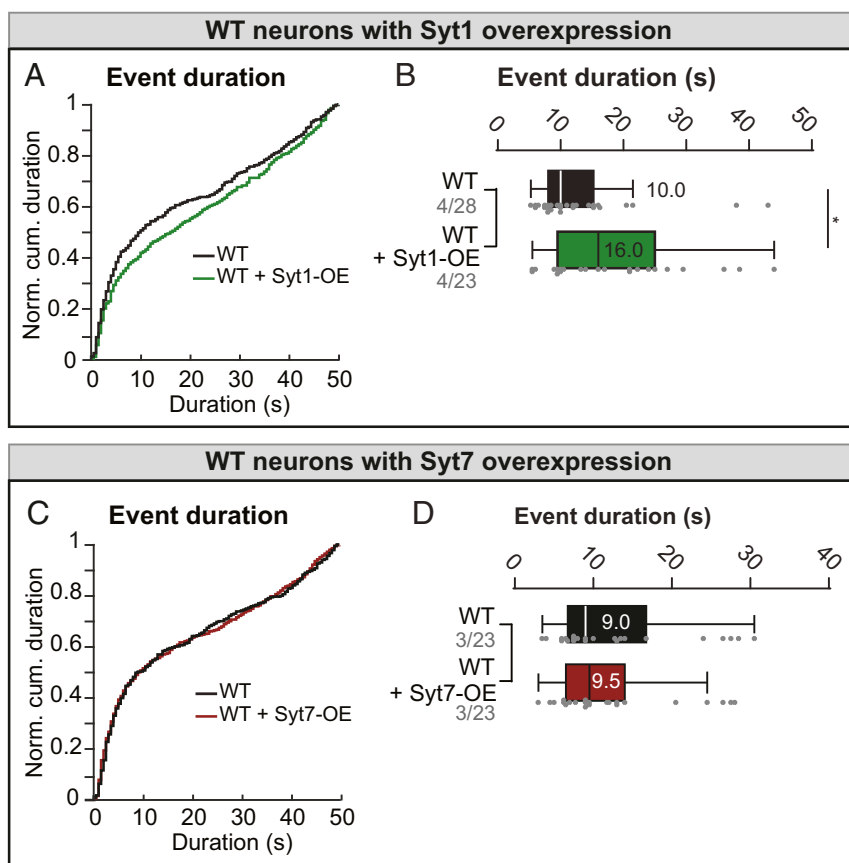
Fig. 7. Syt1-OE, but not Syt7-OE, increases DCV event duration. (A and B) Fusion duration is prolonged in WT neurons with Syt1-OE (Mann–Whitney $U = 218$, $P < 0.05$). (C and D) Fusion event duration is not affected in WT neurons with Syt7-OE (Mann–Whitney $U = 258$, $P = 0.89$). The numbers before and after the dash represent the number of neurites and the number of trafficking vesicles, respectively. All data presented in this figure corresponds to data presented in Fig. 3. *$P < 0.05$, nonsignificant $P > 0.05$.

Ca^{2+} channel accumulation produces rapid local Ca^{2+} transients (67, 68). Hence, it will take longer before Ca^{2+} transients spread through the terminal/axon and activate DCV Ca^{2+} sensors. Since Syt1 is among the Ca^{2+} sensors with the lowest Ca^{2+} sensitivity (15), Ca^{2+} must rise to a high micromolar level before this sensor is activated. This reasoning contributes to an explanation for the slow DCV release onset. However, previous studies indicate a considerable delay between the peak of (bulk) Ca^{2+} increase in axons and the onset of DCV fusion (34). Therefore, additional factors probably contribute to the slow DCV release onset.

Overexpression of Syt1 or Syt7 fully compensated for each other's loss in DCV fusion (cross-rescue, Fig. 2), despite being in different cellular locations (Figs. 4 *A–K* and 5 *B–E*). Hence, the subcellular localization of Ca^{2+} sensors for DCV fusion, and also their different Ca^{2+} sensitivity (9, 15), do not have a major influence on their capacity to support DCV fusion. A similar conclusion was reached for the localization of Syt1 in synaptic vesicle fusion (59, 60).

Syt1 and Syt7 were shown to act as redundant Ca^{2+} sensors for Ca^{2+}-dependent α-amino-3-hydroxy-5-methyl-4-isoxazolepropionic acid receptor (AMPA) receptor exocytosis during the induction of long-term potentiation (69). While loss of either Syt1 or Syt7 was sufficient to lose most DCV fusion events (Figs. 1 *C* and *D* and 2 *A–F* and *SI Appendix*, Figs. S4 *D–H*, S7 *A–F*, and S11 *C, D, I,* and *J*), AMPA receptor insertion was lost only after losing both (69). Hence, native Syt1/7 expression levels are probably more rate limiting for DCV fusion than for AMPA receptor insertion, as WT neurons do not express enough of one Syt to compensate for the loss of the other in single null mutant neurons (Fig. 1 *C* and *D*). This conclusion is further supported by the fact that either Syt1 or

Syt7 overexpression produced substantial (twofold and 1.5-fold, respectively) increase in DCV fusion in WT neurons (Fig. 3 *A–D*). Syt1 messenger RNA levels were not affected after Syt7KD nor did Syt1 levels differ between Syt7 null mutant neurons with and without Syt7 overexpression (20), suggesting neurons do not compensate for the loss of one sensor by increasing expression of the other. Similarly, WT neurons overexpressing either Syt did not result in altered expression of the other (*SI Appendix*, Fig. S5 *C* and *D*). Because Syt1 and Syt7 cellular expression levels are rate limiting for DCV fusion (Fig. 3 *A–D*), at least in hippocampal neurons, transcription regulation of either of the two genes is a powerful way to regulate neuromodulation.

Syt1 deficiency, but not Syt7 deficiency, shortened the duration of DCV fusion events (Fig. 6 *A–H* and *SI Appendix*, Figs. S11 *E, F, K,* and *I* and S12 *C, D, G,* and *H*) in contrast to effects of Syt7 loss in neuroendocrine secretion (56, 70). This is consistent with previous observations of shortened event duration of single SV fusion events in Syt1-KO neurons (51). A shorter event duration may reflect a more rapid fusion pore reclosing (kiss-and-run) or a more rapid pore dilation followed by more rapid cargo diffusion (full fusion). Alternatively, Syt1 deficiency may affect cargo aggregation and subsequently alter the time it takes for the crystalline core to dissolve. However, the main indicator of cargo processing and crystallization, the pH, was not visibly changed in neurons, as Syt1-deficient vesicles were still quenched (Fig. 6*A*). It is therefore likely that Syt1 regulates fusion event duration by affecting pore stability. This is in line with structural studies suggesting that Syt1 Ca^{2+} binding and membrane insertion reorients the SNARE complex to act as a lever that increases fusion pore size (71).

van Westen et al.
Neuromodulator release in neurons requires two functionally redundant calcium sensors

PNAS | 9 of 12
https://doi.org/10.1073/pnas.2012137118

In line with these observations, a Syt1 mutant with a gain-of-function for membrane insertion showed increased fusion pore expansion and cargo release in PC12 cells (72). This suggests that Syt1 requires its membrane interaction to support fusion pore dilation and subsequent cargo release. In principle, alterations in cargo release efficiency because of Syt1 loss may confound pool size estimations. However, these estimations were not significantly different with or without Syt1 (*SI Appendix*, Fig. S5*A*).

Syt1 overexpression increased fusion event duration in WT neurons (Fig. 7 *A–D*) but not in Syt7-KO neurons. (Fig. 6 *G* and *H*). This suggests that Syt1 is sufficient to prolong fusion pore opening but requires Syt7. The unique properties of Syt7 appear to be a prerequisite for Syt1 to promote fusion pore open duration. Finally, GAP43-Syt1 fully rescued DCV fusion but not fusion event duration, whereas GAP43-Syt7 did not (*SI Appendix*, Fig. S11 *A–I*). Together, this suggests that the pore duration, but not the pore opening, requires the luminal/transmembrane domain of Syt1, possibly for a correct Syt1 topology.

The fact that Syt1, but not Syt7, regulates fusion event duration suggests that Syt1 acts downstream of Syt7 in DCV secretion. Unlike other secretory pathways, especially in synapses and chromaffin cells, the sequence of events is still poorly defined, and the molecules characterized only partially. At the fusion step, multiple R-SNAREs (73, 74) may work with SNAP25 (73, 75), but the Qa SNARE (syntaxin paralog) and SM-protein (Munc18 paralog) are unknown. The Rab3A/RIM/Munc13 complex is essential (76) and may act upstream of the SNAREs. The fact that Syt1 regulates DCV fusion event duration suggests that at least one role of Syt1 is downstream of the action of all these molecules. It is quite plausible that both Syts have additional roles as demonstrated for the synaptic vesicle and chromaffin granule pathways (77, 78). Syt7 has been suggested to facilitate priming, contributing to the fast phase of secretion in neuroendocrine secretion (21). In contrast to SVs or chromaffin granules (CGs), we currently have no way of defining the readily releasable pool for neuronal DCVs (no protocol/stimulus to define the release-ready DCV pool like hyperosmotic sucrose for SVs or Ca^{2+} flash for CGs). Therefore, the "primed" state/pool is not yet defined for DCVs either. Better definitions of DCV pools and their release probabilities (34) are required to define better working models for the DCV pathway and the molecular function(s) of Syt1 and Syt7.

Materials and Methods

Animals. Primary hippocampal cultures were prepared from Doc2ab-DKO and DHzs littermates, or Syt1-KO, Syt7-KO C57BL/6J mice with WT littermates, of both sexes. Doc2a/b-DKO animals were previously described (35). Syt1-KO (8) and Syt7-KO animals (44) were a kind gift from Thomas C. Südhof, Stanford University, Stanford, CA. Syt heterozygous animals were crossbred to generate WT and KO littermate pups for culturing. Animals were genotyped at E18 (Syt1) or P0 (Syt7 and Doc2a/b) prior to culturing. All animals were bred and housed in line with institutional and Dutch governmental guidelines, and all procedures were approved by the ethical committee of the Vrije Universiteit, Amsterdam, The Netherlands (DEC-FGA 11-03 and AVD112002017824).

Primary Neuronal Cultures. Primary cultures were prepared as described previously (40). For more details, see *SI Appendix*.

Constructs and Infections. hNPY-SEP and hNPY-mCherry were made by replacement of NPY-Venus (79) with SEP or mCherry. NPY-SEP is used for all experiments with the exception of those presented in Fig. 5 and *SI Appendix*, Fig. S8. See *SI Appendix, Supplementary Methods* for a detailed explanation and rationale on the two constructs. Syt1 open reading frame and Syt1–short hairpin RNA were a kind gift from T. C. Südhof (43). Mouse copy DNA was prepared from the short (403 amino acid [aa], Ensembl Syt7-201) splice variant of Syt7 and sequenced. Syt1 and Syt7 were cloned into a lentivirus backbone, additionally encoding a nuclear-targeted mCherry signal. To generate Ca^{2+}-binding mutant Syts (Syt1-DA and Syt7-DA), Ca^{2+}-binding aspartates were substituted for alanines as described previously (20). Fluorescent-Syt fusion constructs were made by cloning a fluorescent protein (mCherry or SEP) to the N terminus of Syt1 and Syt7, preceded by a preprotachykinin signal peptide to

ensure endoplasmic reticulum targeting [kind gift from Jakob B. Sørensen, University of Copenhagen, Copenhagen, Denmark (80)]. GAP43-Syt1, encoding GAP43 1 to 41 aa fused to the N terminus of Syt1 96 to 422 aa, was a kind gift from Edwin R. Chapman, University of Wisconsin, Madison, WI (59, 60). GAP43-Syt7 was generated by fusing the coding sequence of GAP43 1 to 41 aa to Syt7 41 to 403 aa. All constructs were driven by a Synapsin promoter, sequence verified and cloned into a pLenti vector and produced as described (81). Syt1-KD and Syt-rescue constructs were applied to neuronal cultures at DIV2. All other infections were performed at DIV10.

Live-Cell Imaging. Live-cell imaging was performed at DIV15 to 20. Microscope hardware, software, and imaging solutions are described in *SI Appendix*. Field stimulation electrodes delivered 16 trains of 50 AP at 50 Hz with 500-ms intervals. No stimulation was used for Syt localization (Fig. 4 *E–H*) and co-traveling experiments (Fig. 4 *I–K*). Cultures were kept at room temperature (21 to 24 °C) perfused with Tyrode's solution. A 10-s exposure to Tyrode's NH4 was used to dequench SEP at the end of each stimulation. For visualization purposes, brightness and contrast of representative examples were adjusted linearly and equally between groups.

Immunocytochemistry. Immunostainings were performed using standard procedures (*SI Appendix*).

Imaging Analysis. In ImageJ, regions of interest (ROIs) of 3 × 3 pixels (equals 0.6 × 0.6 µm) were placed manually on SEP fusion events, somatic events not included. Movement of dequenched vesicles out of the ROIs in X/Y direction is very rare but was detected by an expert observer during validation of the ROI placements in the image stack (movie) and lead to repositioning or cancellation of the ROI. ROI intensity measures were exported to MATLAB for semiautomated detection of fusion events and duration. Intensity traces were plotted as $\Delta F/F_0$, with the average fluorescence of the first 10 frames used to determine F_0. Events were defined as a sudden increase of 2 SD above F_0. Pool estimation was performed using SynD software (82) in MATLAB. For this, a neurite mask (soma not included) was drawn in SynD to estimate the number of puncta/DCVs. Detection parameters were optimized to detect vesicle puncta and kept constant during all datasets. For each neuron, the intensity of an individual DCV was estimated by taking the fluorescence intensity mode per cell in the first two quantiles. Pool size was estimated by correcting the puncta intensities on the individual DCV intensity. Manders overlap coefficient (M1/M2) was determined on neurites exclusively, including above threshold fluorescence as determined in ImageJ using the JACoP plugin (83). The Mander's coefficient can be defined as the fraction of total signal in one channel that overlaps/co-occurs with (above threshold) signal of the other channel: 0 representing no overlap, and 1 indicating complete overlap.

Statistics. Data that violated normality (D'Agostino–Pearson) and homogeneity (Fligner-Killeen) was tested with the two-sided Mann–Whitney U test or Kruskal–Wallis (generating a U-statistic and X^2-statistic, respectively) and Dunn's multiple comparison with the Benjamini–Hochberg correction. For cumulative plots, the cumulative median number of events were taken for each time point for each neuron. Box plots were plotted with 25 and 75% interquartile range and Tukey whiskers, presenting the median value in or next to the box plot. The number before and after the dash represents the number of independent experiments and the number of neurons, respectively. When assumptions of homogeneity and normality were met, data were tested with Student's t test or one-way ANOVA and the Holm–Sidak correction and plotted as mean ± SEM. N represents the number of litters, and n represents the number of individual neurons, unless stated otherwise.

Western Blotting. Western blots were performed using standard procedures (*SI Appendix*).

Data Availability. The code and data generated during the current study have been submitted to the Dataverse online repository (DOI: 10.34894/BGJAXY) (84).

10 of 12 | PNAS
https://doi.org/10.1073/pnas.2012137118

van Westen et al.
Neuromodulator release in neurons requires two functionally redundant calcium sensors

1. S. J. Smith et al., Single-cell transcriptomic evidence for dense intracortical neuro-peptide networks. eLife 8, e47889 (2019).
2. A. N. van den Pol, Neuropeptide transmission in brain circuits. Neuron 76, 98–115 (2012).
3. M. M. Poo, Neurotrophins as synaptic modulators. Nat. Rev. Neurosci. 2, 24–32 (2001).
4. M. J. Zaben, W. P. Gray, Neuropeptides and hippocampal neurogenesis. Neuropeptides 47, 431–438 (2013).
5. V. Kormos, B. Gaszner, Role of neuropeptides in anxiety, stress, and depression: From animals to humans. Neuropeptides 47, 401–419 (2013).
6. S. Kovac, M. C. Walker, Neuropeptides in epilepsy. Neuropeptides 47, 467–475 (2013).
7. S. O. Ogren, E. Kuteeva, E. Elvander-Tottie, T. Hökfelt, Neuropeptides in learning and memory processes with focus on galanin. Eur. J. Pharmacol. 626, 9–17 (2010).
8. M. Geppert et al., Synaptotagmin I: A major Ca2+ sensor for transmitter release at a central synapse. Cell 79, 717–727 (1994).
9. C. Li et al., Ca(2+)-dependent and -independent activities of neural and non-neural synaptotagmins. Nature 375, 594–599 (1995).
10. M. S. Perin, V. A. Fried, G. A. Mignery, R. Jahn, T. C. Südhof, Phospholipid binding by a synaptic vesicle protein homologous to the regulatory region of protein kinase C. Nature 345, 260–263 (1990).
11. C. von Poser, K. Ichtchenko, X. Shao, J. Rizo, T. C. Südhof, The evolutionary pressure to inactivate. A subclass of synaptotagmins with an amino acid substitution that abol-ishes Ca2+ binding. J. Biol. Chem. 272, 14314–14319 (1997).
12. M. Craxton, Synaptotagmin gene content of the sequenced genomes. BMC Genomics 5, 43 (2004).
13. M. Craxton, Evolutionary genomics of plant genes encoding N-terminal-TM-C2 do-main proteins and the similar FAM62 genes and synaptotagmin genes of metazoans. BMC Genomics 8, 259 (2007).
14. A. Bhalla, M. C. Chicka, E. R. Chapman, Analysis of the synaptotagmin family during reconstituted membrane fusion. Uncovering a class of inhibitory isoforms. J. Biol. Chem. 283, 21799–21807 (2008).
15. S. Sugita, O.-H. Shin, W. Han, Y. Lao, T. C. Südhof, Synaptotagmins form a hierarchy of exocytotic Ca(2+) sensors with distinct Ca(2+) affinities. EMBO J. 21, 270–280 (2002).
16. E. Hui et al., Three distinct kinetic groupings of the synaptotagmin family: Candidate sensors for rapid and delayed exocytosis. Proc. Natl. Acad. Sci. U.S.A. 102, 5210–5214 (2005).
17. S. L. Jackman, W. G. Regehr, The mechanisms and functions of synaptic facilitation. Neuron 94, 447–464 (2017).
18. T. Voets et al., Intracellular calcium dependence of large dense-core vesicle exocytosis in the absence of synaptotagmin I. Proc. Natl. Acad. Sci. U.S.A. 98, 11680–11685 (2001).
19. A. Banerjee, J. Lee, P. Nemcova, C. Liu, P. S. Kaeser, Synaptotagmin-1 is the Ca^{2+} sensor for fast striatal dopamine release. eLife 9, e58359 (2020).
20. T. Bacaj et al., Synaptotagmin-1 and synaptotagmin-7 trigger synchronous and asynchronous phases of neurotransmitter release. Neuron 80, 947–959 (2013).
21. J.-S. Schonn, A. Maximov, Y. Lao, T. C. Südhof, J. B. Sørensen, Synaptotagmin-1 and -7 are functionally overlapping Ca2+ sensors for exocytosis in adrenal chromaffin cells. Proc. Natl. Acad. Sci. U.S.A. 105, 3998–4003 (2008).
22. Z. Gao, J. Reavey-Cantwell, R. A. Young, P. Jegier, B. A. Wolf, Synaptotagmin III/VII isoforms mediate Ca2+-induced insulin secretion in pancreatic islet beta-cells. J. Biol. Chem. 275, 36079–36085 (2000).
23. B. R. Gauthier et al., Synaptotagmin VII splice variants α, β, and δ are expressed in pancreatic β-cells and regulate insulin exocytosis. FASEB J. 22, 194–206 (2008).
24. N. Gustavsson et al., Impaired insulin secretion and glucose intolerance in synaptotagmin-7 null mutant mice. Proc. Natl. Acad. Sci. U.S.A. 105, 3992–3997 (2008).
25. C. Dean et al., Synaptotagmin-IV modulates synaptic function and long-term poten-tiation by regulating BDNF release. Nat. Neurosci. 12, 767–776 (2009).
26. G. Zhang et al., Neuropeptide exocytosis involving synaptotagmin-4 and oxytocin in hypothalamic programming of body weight and energy balance. Neuron 69, 523–535 (2011).
27. L. K. Roper, J. S. Briguglio, C. S. Evans, M. B. Jackson, E. R. Chapman, Sex-specific regulation of follicle-stimulating hormone secretion by synaptotagmin 9. Nat. Commun. 6, 8645 (2015).
28. M. Fukuda, J. A. Kowalchyk, X. Zhang, T. F. Martin, K. Mikoshiba, Synaptotagmin IX regulates Ca2+-dependent secretion in PC12 cells. J. Biol. Chem. 277, 4601–4604 (2002).
29. K. L. Lynch, T. F. J. Martin, Synaptotagmins I and IX function redundantly in regulated exocytosis but not endocytosis in PC12 cells. J. Cell Sci. 120, 617–627 (2007).
30. P. Cao, A. Maximov, T. C. Südhof, Activity-dependent IGF-1 exocytosis is controlled by the Ca(2+)-sensor synaptotagmin-10. Cell 145, 300–311 (2011).
31. T. Mittelsteadt et al., Differential mRNA expression patterns of the synaptotagmin gene family in the rodent brain. J. Comp. Neurol. 512, 514–528 (2009).
32. J. Xu, T. Mashimo, T. C. Südhof, Synaptotagmin-1, -2, and -9: Ca(2+) sensors for fast release that specify distinct presynaptic properties in subsets of neurons. Neuron 54, 567–581 (2007).
33. A. Zeisel et al., Brain structure. Cell types in the mouse cortex and hippocampus re-vealed by single-cell RNA-seq. Science 347, 1138–1142 (2015).
34. C. M. Persoon et al., Pool size estimations for dense-core vesicles in mammalian CNS neurons. EMBO J. 37, 99672 (2018).
35. A. J. Groffen et al., Doc2b is a high-affinity Ca2+ sensor for spontaneous neuro-transmitter release. Science 327, 1614–1618 (2010).
36. Z. P. Pang et al., Doc2 supports spontaneous synaptic transmission by a Ca(2+)-inde-pendent mechanism. Neuron 70, 244–251 (2011).
37. M. Verhage et al., DOC2 proteins in rat brain: Complementary distribution and pro-posed function as vesicular adapter proteins in early stages of secretion. Neuron 18, 453–461 (1997).
38. J. Yao, J. D. Gaffaney, S. E. Kwon, E. R. Chapman, Doc2 is a Ca2+ sensor required for asynchronous neurotransmitter release. Cell 147, 666–677 (2011).
39. R. van de Bospoort et al., Munc13 controls the location and efficiency of dense-core vesicle release in neurons. J. Cell Biol. 199, 883–891 (2012).
40. J. Emperador-Melero et al., Vti1a/b regulate synaptic vesicle and dense core vesicle secretion via protein sorting at the Golgi. Nat. Commun. 9, 3421 (2018).
41. J. de Wit, R. F. Toonen, M. Verhage, Matrix-dependent local retention of secretory vesicle cargo in cortical neurons. J. Neurosci. 29, 23–37 (2009).
42. A. J. A. Groffen, R. Friedrich, E. C. Brian, U. Ashery, M. Verhage, DOC2A and DOC2B are sensors for neuronal activity with unique calcium-dependent and kinetic prop-erties. J. Neurochem. 97, 818–833 (2006).
43. W. Xu et al., Distinct neuronal coding schemes in memory revealed by selective era-sure of fast synchronous synaptic transmission. Neuron 73, 990–1001 (2012).
44. A. Maximov et al., Genetic analysis of synaptotagmin-7 function in synaptic vesicle exocytosis. Proc. Natl. Acad. Sci. U.S.A. 105, 3986–3991 (2008).
45. N. Brose, A. G. Petrenko, T. C. Südhof, R. Jahn, Synaptotagmin: A calcium sensor on the synaptic vesicle surface. Science 256, 1021–1025 (1992).
46. W. D. Matthew, L. Tsavaler, L. F. Reichardt, Identification of a synaptic vesicle-specific membrane protein with a wide distribution in neuronal and neurosecretory tissue. J. Cell Biol. 91, 257–269 (1981).
47. S. Takamori et al., Molecular anatomy of a trafficking organelle. Cell 127, 831–846 (2006).
48. C. Dean et al., Axonal and dendritic synaptotagmin isoforms revealed by a pHluorin-syt functional screen. Mol. Biol. Cell 23, 1715–1727 (2012).
49. H. Liu et al., Synaptotagmin 7 functions as a Ca2+-sensor for synaptic vesicle re-plenishment. eLife 3, e01524 (2014).
50. M. Wienisch, J. Klingauf, Vesicular proteins exocytosed and subsequently retrieved by compensatory endocytosis are nonidentical. Nat. Neurosci. 9, 1019–1027 (2006).
51. Y. C. Li, N. L. Chanaday, W. Xu, E. T. Kavalali, Synaptotagmin-1- and synaptotagmin-7-dependent fusion mechanisms target synaptic vesicles to kinetically distinct endocytic pathways. Neuron 93, 616–631.e3 (2016).
52. N. R. Gandasi et al., Survey of red fluorescence proteins as markers for secretory granule exocytosis. PLoS One 10, e0127901 (2015).
53. C.-T. Wang et al., Synaptotagmin modulation of fusion pore kinetics in regulated exocytosis of dense-core vesicles. Science 294, 1111–1115 (2001).
54. C.-T. Wang, J. Bai, P. Y. Chang, E. R. Chapman, M. B. Jackson, Synaptotagmin-Ca2+ triggers two sequential steps in regulated exocytosis in rat PC12 cells: Fusion pore opening and fusion pore dilation. J. Physiol. 570, 295–307 (2006).
55. J. Bai, C.-T. Wang, D. A. Richards, M. B. Jackson, E. R. Chapman, Fusion pore dynamics are regulated by synaptotagmin*t-SNARE interactions. Neuron 41, 929–942 (2004).
56. M. Segovia et al., Push-and-pull regulation of the fusion pore by synaptotagmin-7. Proc. Natl. Acad. Sci. U.S.A. 107, 19032–19037 (2010).
57. Z. Zhang, E. Hui, E. R. Chapman, M. B. Jackson, Regulation of exocytosis and fusion pores by synaptotagmin-effector interactions. Mol. Biol. Cell 21, 2821–2831 (2010).
58. M. Bendahmane et al., The synaptotagmin C2B domain calcium-binding loops mod-ulate the rate of fusion pore expansion. Mol. Biol. Cell 29, 834–845 (2018).
59. J. Yao, S. E. Kwon, J. D. Gaffaney, F. M. Dunning, E. R. Chapman, Uncoupling the roles of synaptotagmin I during endo- and exocytosis of synaptic vesicles. Nat. Neurosci. 15, 243–249 (2011).
60. E. Hui, C. P. Johnson, J. Yao, F. M. Dunning, E. R. Chapman, Synaptotagmin-mediated bending of the target membrane is a critical step in Ca(2+)-regulated fusion. Cell 138, 709–721 (2009).
61. I. Martinez et al., Synaptotagmin VII regulates Ca(2+)-dependent exocytosis of lyso-somes in fibroblasts. J. Cell Biol. 148, 1141–1149 (2000).
62. N. Gustavsson et al., Synaptotagmin-7 is a principal Ca2+ sensor for Ca2+ -induced glucagon exocytosis in pancreas. J. Physiol. 587, 1169–1178 (2009).
63. M. Iezzi, G. Kouri, M. Fukuda, C. B. Wollheim, Synaptotagmin V and IX isoforms control Ca2+ -dependent insulin exocytosis. J. Cell Sci. 117, 3119–3127 (2004).
64. M. Vrljic et al., Molecular mechanism of the synaptotagmin-SNARE interaction in Ca2+-triggered vesicle fusion. Nat. Struct. Mol. Biol. 17, 325–331 (2010).
65. T. Bacaj et al., Synaptotagmin-1 and -7 are redundantly essential for maintaining the capacity of the readily-releasable pool of synaptic vesicles. PLoS Biol. 13, e1002267 (2015).
66. C. Imig et al., The morphological and molecular nature of synaptic vesicle priming at presynaptic active zones. Neuron 84, 416–431 (2014).
67. R. Llinás, M. Sugimori, R. B. Silver, Microdomains of high calcium concentration in a presynaptic terminal. Science 256, 677–679 (1992).
68. R. S. Zucker, A. L. Fogelson, Relationship between transmitter release and presynaptic calcium influx when calcium enters through discrete channels. Proc. Natl. Acad. Sci. U.S.A. 83, 3032–3036 (1986).
69. D. Wu et al., Postsynaptic synaptotagmins mediate AMPA receptor exocytosis during LTP. Nature 544, 316–321 (2017).
70. T. C. Rao et al., Distinct fusion properties of synaptotagmin-1 and synaptotagmin-7 bearing dense core granules. Mol. Biol. Cell 25, 2416–2427 (2014).
71. Z. Wu, N. Dharan, S. Thiyagarajan, B. O'Shaughnessy, E. Karatekin, The neuronal calcium sensor synaptotagmin-1 and SNARE proteins cooperate to dilate fusion pores mechanically. bioRxiv [Preprint] (2019). https://doi.org/10.1101/623827 (Accessed 13 July 2020).
72. K. L. Lynch et al., Synaptotagmin-1 utilizes membrane bending and SNARE binding to drive fusion pore expansion. Mol. Biol. Cell 19, 5093–5103 (2008).
73. M. Shimojo et al., SNAREs controlling vesicular release of BDNF and development of callosal axons. Cell Rep. 11, 1054–1066 (2015).

van Westen et al.
Neuromodulator release in neurons requires two functionally redundant calcium sensors

PNAS | 11 of 12
https://doi.org/10.1073/pnas.2012137118

74. R. I. Hoogstraaten, L. van Keimpema, R. F. Toonen, M. Verhage, Tetanus insensitive VAMP2 differentially restores synaptic and dense core vesicle fusion in tetanus neurotoxin treated neurons. *Sci. Rep.* **10**, 10913 (2020).

75. S. Arora *et al*., SNAP-25 gene family members differentially support secretory vesicle fusion. *J. Cell Sci.* **130**, 1877–1889 (2017).

76. C. M. Persoon *et al*., The RAB3-RIM pathway is essential for the release of neuromodulators. *Neuron* **104**, 1065–1080.e12 (2019).

77. H. de Wit *et al*., Synaptotagmin-1 docks secretory vesicles to syntaxin-1/SNAP-25 acceptor complexes. *Cell* **138**, 935–946 (2009).

78. S. Chang, T. Trimbuch, C. Rosenmund, Synaptotagmin-1 drives synchronous Ca^{2+}-triggered fusion by C_2B-domain-mediated synaptic-vesicle-membrane attachment. *Nat. Neurosci.* **21**, 33–40 (2018).

79. T. Nagai *et al*., A variant of yellow fluorescent protein with fast and efficient maturation for cell-biological applications. *Nat. Biotechnol.* **20**, 87–90 (2002).

80. J. P. Weber, T. L. Toft-Bertelsen, R. Mohrmann, I. Delgado-Martinez, J. B. Sørensen, Synaptotagmin-7 is an asynchronous calcium sensor for synaptic transmission in neurons expressing SNAP-23. *PLoS One* **9**, e114033 (2014).

81. L. Naldini, U. Blömer, F. H. Gage, D. Trono, I. M. Verma, Efficient transfer, integration, and sustained long-term expression of the transgene in adult rat brains injected with a lentiviral vector. *Proc. Natl. Acad. Sci. U.S.A.* **93**, 11382–11388 (1996).

82. S. K. Schmitz *et al*., Automated analysis of neuronal morphology, synapse number and synaptic recruitment. *J. Neurosci. Methods* **195**, 185–193 (2011). Corrected in: *J. Neurosci. Methods* **197**, 190 (2011).

83. S. Bolte, F. P. Cordelières, A guided tour into subcellular colocalization analysis in light microscopy. *J. Microsc.* **224**, 213–232 (2006).

84. R. van Westen *et al*., Neuromodulator release in neurons requires two functionally redundant calcium sensors. DataVerseNL. https://dataverse.nl/dataset.xhtml?persistentId=doi:10.34894/BGJAXY. Deposited 24 December 2020.